

Nonstoichiometry (δ) and High-Temperature Thermodynamic Properties of $(\text{Mg}_{0.22}\text{Mn}_{0.07}\text{Fe}_{0.71})_{3-\delta}\text{O}_4$ Ferrite Spinel

Sun-Ho Kang and Han-Ill Yoo¹

School of Materials Science and Engineering, Seoul National University, Seoul 151-742, Korea

Received November 25, 1998; accepted February 24, 1999

Nonstoichiometry of $(\text{Mg}_{0.22}\text{Mn}_{0.07}\text{Fe}_{0.71})_{3-\delta}\text{O}_4$ ferrite has been measured in the temperature range of 1000–1200°C as a function of oxygen activity (a_{O_2}) using a solid state coulometric titration technique. At a given temperature, the nonstoichiometry (δ) was found to vary with the oxygen activity as $\delta = [V]^0 \cdot a_{\text{O}_2}^{2/3} - [I]^0 \cdot a_{\text{O}_2}^{-2/3}$ where $[V]^0$ and $[I]^0$ are constants. This a_{O_2} -dependence of δ was explained in terms of Frenkel disorder, i.e., cation vacancy and interstitial. From the temperature dependence of the defect constants ($[V]^0$ and $[I]^0$) and the oxygen activity for the stoichiometric composition ($\delta=0$), thermodynamic quantities such as enthalpies for the defect formation reactions and relative partial molar enthalpy and entropy of oxygen were calculated. © 1999 Academic Press

Key Words: $(\text{Mg}_{0.22}\text{Mn}_{0.07}\text{Fe}_{0.71})_{3-\delta}\text{O}_4$ ferrite; Nonstoichiometry; Solid state coulometric titration; Frenkel disorder.

INTRODUCTION

Spinel ferrites (Me, Fe) $_{3-\delta}\text{O}_4$ ($\text{Me} = \text{Mg}, \text{Mn}, \text{MgMn}, \text{MnZn}, \text{etc.}$) are stable over a range of oxygen activity, a_{O_2} ($\equiv P_{\text{O}_2}/\text{atm}$), at elevated temperatures (1–6). Metal-to-oxygen ratio, or nonstoichiometry (δ), of the spinel ferrites varies depending on the oxygen activity during sintering and cooling process in ferrite fabrication. The metal deficit or excess arising from the nonstoichiometry is compensated by the oxidation or reduction of transition metal ions, e.g., Mn and Fe. The electrical and magnetic properties of spinel ferrites originate from the spin states of the transition metal ions and the interactions among the ions located at tetrahedral and octahedral interstices in the spinel structure (7). Therefore, the nonstoichiometry (δ) of a spinel ferrite (Me, Fe) $_{3-\delta}\text{O}_4$, as a direct measure of average oxidation states of transition metal ions and point defect concentrations, is one of the crucial factors to control in tailoring the electromagnetic properties of the ferrite at elevated, processing temperatures (7–11).

¹To whom correspondence should be addressed. Fax: 82-2-884-1413. E-mail: hiyoo@plaza.snu.ac.kr.

In the present work, the nonstoichiometry (δ) of $(\text{Mg}_{0.22}\text{Mn}_{0.07}\text{Fe}_{0.71})_{3-\delta}\text{O}_4$ ferrite, an important magnetic material particularly for high-frequency applications due to its high electrical resistivity (12, 13), has been measured as a function of oxygen activity, a_{O_2} , in the temperature range of 1000–1200°C by a solid state coulometric titration technique. Thermodynamic quantities, such as enthalpy changes of defect formation reactions and the relative partial molar enthalpy and entropy of oxygen, have been extracted from the temperature dependence of the nonstoichiometry.

EXPERIMENTAL

Sample Preparation

$(\text{Mg}_{0.22}\text{Mn}_{0.07}\text{Fe}_{0.71})_{3-\delta}\text{O}_4$ ferrite, was prepared from the starting powders of MgO (99.99%, High Purity Chemicals, Japan), Mn_3O_4 (9.9%, MMC, South Africa), and Fe_2O_3 (99.99%, High Purity Chemicals) via a conventional ceramic processing route. Sintering was carried out at 1350°C in air atmosphere for 4 h. The exact cationic composition was determined by ICP-emission spectrophotometry. Average grain size and apparent density were $12 \pm 7 \mu\text{m}$ and 97.7% of theoretical density, respectively.

Construction of Electrochemical Cell

Coulometric titration cells were constructed as schematically shown in Fig. 1. As a solid electrolyte (8 in the figure), a disk of 8 mol% $\text{Y}_2\text{O}_3\text{-ZrO}_2$ Solid solution (8YSZ), 12.5 mm diameter \times (1.0–1.5) mm thick was used. The disk was polished on both planar surfaces with assorted diamond pastes of grit size down to 1 μm . As a gas electrode (11 in the figure), a piece of Pt gauze (29809-3, 100 mesh, Aldrich) measuring 2.5×2.5 mm, was subsequently attached to each polished surface of the YSZ disk with the aid of Pt paste (5542, unfluxed, Engelhard) by firing overnight at about 1300°C in air atmosphere.

An alumina cup (4 in Fig. 1), measuring 10.5 mm o.d. \times 8 mm i.d. \times (3–4) mm high, served as a chamber to carry

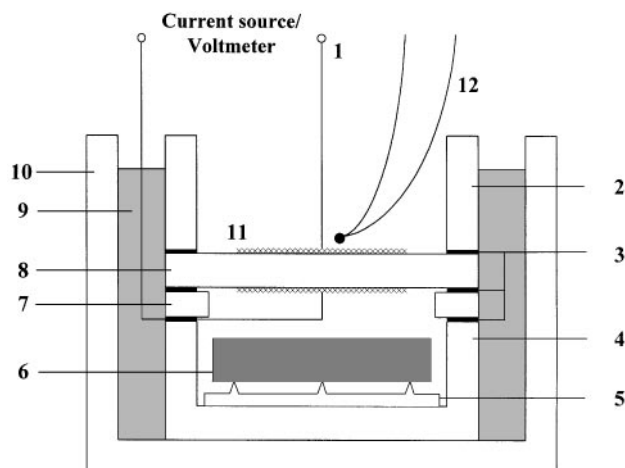


FIG. 1. Schematic view of the electrochemical cell. 1, Pt-lead wire; 2, YSZ ring; 3, Pt-foil; 4, alumina cup; 5, alumina needles; 6, specimen; 7, alumina ring; 8, YSZ disk; 9, silicate glass; 10, alumina crucible; 11, Pt-gauze; 12, S-type thermocouple.

a ferrite specimen (6 in the figure) inside. The ferrite specimen was placed upon alumina needles (5 in the figure), which were employed to minimize possible reactions between alumina and the ferrite specimen.

In stacking the disk of electrolyte upon the sample chamber, an alumina ring (7 in Fig. 1), 10 mm o.d. \times 8 mm i.d. \times 1 mm thick, was inserted for the purpose of electrical insulation between the Pt-lead wire and the bare surface of the electrolyte. The Pt-lead wire was brought out of the cell between the alumina ring and alumina cup via a Pt ring (3 in the figure).

The as-assembled titration cell was placed inside an alumina crucible (10 in Fig. 1), 26 mm i.d. \times (18–20) mm high, and the empty space between the cell and the crucible was filled with silicate glass powder (9 in the figure) whose composition was 49 wt% SiO_2 , 25 wt% BaO , 16 wt% B_2O_3 , and 10 wt% Al_2O_3 . At elevated temperatures, glass powder melted to provide a satisfactory gas-tight seal.

Coulometric Titration

Constant current, I , was passed through the YSZ electrolyte for a predetermined period of time, t , by using a d.c. current source (Keithley 224). The amount of molecular oxygen, ΔN_{O_2} , which was removed from or added to the sample chamber can be written as

$$\Delta N_{\text{O}_2} = \frac{I \cdot t}{4F}, \quad [1]$$

where F is the Faraday constant. As the dead volume of the titration cell is made sufficiently small in the present work (14, 15), ΔN_{O_2} can be assumed to be equal to the change in

the number of oxygen molecule in the ferrite sample. When the nonstoichiometry of n mole of $\text{M}_{3-\delta}\text{O}_4$, such as $\text{Mn}_{3-\delta}\text{O}_4$, $\text{Fe}_{3-\delta}\text{O}_4$, and $\text{Co}_{3-\delta}\text{O}_4$, is changed from δ^* to δ by the titration procedure, ΔN_{O_2} is given in terms of δ^* and δ as

$$\begin{aligned} \Delta N_{\text{O}_2} &= \frac{3n}{2} \left(\frac{4}{3-\delta} - \frac{4}{3-\delta^*} \right) \\ &= \frac{2n}{3} \frac{\Delta\delta}{(1-\delta/3)(1-\delta^*/3)}, \end{aligned} \quad [2]$$

where $\Delta\delta = \delta - \delta^*$. With the assumption that $\delta/3, \delta^*/3 \ll 1$, the change of the nonstoichiometry ($\Delta\delta$) can be expressed as

$$\Delta\delta = \frac{3M_o}{2m_o} \Delta N_{\text{O}_2} = \frac{3M_o I t}{8m_o F}, \quad [3]$$

where M_o and m_o are the molar weight of $(\text{Mg}_{0.22}\text{Mn}_{0.07}\text{Fe}_{0.71})_{3-\delta}\text{O}_4$ and the initial (i.e., before titration) weight of the specimen, respectively. Consequently, the nonstoichiometry of $(\text{Mg}_{0.22}\text{Mn}_{0.07}\text{Fe}_{0.71})_{3-\delta}\text{O}_4$ can be controlled by passing a known amount of electric charge ($I \cdot t$ coulombs) through the solid electrolyte.

After the current was turned off, the open-circuit e.m.f. across the YSZ electrolyte was monitored with a digital multimeter (Keithley 197) to determine the equilibrium oxygen activity over the specimen, a_{O_2} , via the Nernst equation,

$$a_{\text{O}_2} = a_{\text{O}_2}^{\text{ref}} \exp \left(- \frac{4EF}{RT} \right), \quad [4]$$

where E is the steady state open-circuit e.m.f. and $a_{\text{O}_2}^{\text{ref}}$ the oxygen activity of the reference gas flowing outside the titration cell. In the present experiment, N_2/O_2 or CO_2/CO mixtures were employed as the reference gas, whose oxygen activity, $a_{\text{O}_2}^{\text{ref}}$, was determined with an oxygen concentration cell based on stabilized zirconia.

RESULTS

By the titration procedure described above, the nonstoichiometry relative to a reference point ($\Delta\delta$) has been determined as a function of oxygen activity (a_{O_2}) within the single phase field of $(\text{Mg}_{0.22}\text{Mn}_{0.07}\text{Fe}_{0.71})_{3-\delta}\text{O}_4$ ferrite (5) at 1000, 1100, and 1200°C, respectively. The experimental results, $\Delta\delta$ vs $\log a_{\text{O}_2}$, are listed in Table 1.

DISCUSSION

Nonstoichiometry (δ) of $(\text{Mg}_{0.22}\text{Mn}_{0.07}\text{Fe}_{0.71})_{3-\delta}\text{O}_4$

In a coulometric titration experiment, relative nonstoichiometry to a reference value (δ^*), i.e., $\Delta\delta = \delta - \delta^*$, is

TABLE 1
 $\Delta\delta$ and δ as a Function of Oxygen Activity (a_{O_2}) in $(Mg_{0.22}Mn_{0.07}Fe_{0.71})_{3-\delta}O_4$ at (a) 1000°C, (b) 1100°C, and (c) 1200°C

(a) $T = 1000^\circ\text{C}$			(b) $T = 1100^\circ\text{C}$			(c) $T = 1200^\circ\text{C}$					
$\log a_{O_2}$	$\Delta\delta$	δ^a	$\log a_{O_2}$	$\Delta\delta$	δ^a	$\log a_{O_2}$	$\Delta\delta$	δ^a	$\log a_{O_2}$	$\Delta\delta$	δ^a
-2.173	0.01	0.0113	-1.351	0.0087	0.0097	-0.967	0	0.0096	-2.364	-0.009	0.0006
-2.281	0.0087	0.0100	-1.538	0.0067	0.0077	-1.067	-0.00124	0.00836	-2.930	-0.00924	0.00360
-2.514	0.005	0.0063	-1.799	0.0047	0.0057	-1.067	-0.00228	0.00732	-3.236	-0.01024	-0.00064
-2.588	0.0057	0.0070	-2.067	0.0027	0.0037	-1.289	-0.00428	0.00532	-4.143	-0.01178	-0.00218
-3.006	0.0027	0.0040	-2.468	0.0007	0.0017	-1.495	-0.005	0.00460	-4.412	-0.01378	-0.00418
-3.217	0.0017	0.0030	-3.402	0	0.0010	-1.631	-0.00628	0.00332	-4.720	-0.01678	-0.00718
-3.481	0.0007	0.0020	-5.730	-0.003	-0.002	-1.711	-0.00624	0.00336	-5.227	-0.02178	-0.01218
-3.710	0	0.0013	-6.870	-0.006	-0.005	-2.071	-0.008	0.00160	-5.416	-0.02678	-0.01718
-3.834	-0.0003	0.001				-2.115	-0.00828	0.00132	-5.470	-0.03178	-0.02218
-5.620	-0.003	-0.017				-2.236	-0.00878	0.00082			
-9.160	-0.005	-0.0037									

^a δ values were calculated with $\Delta\delta$ in this table and δ^* in Table 2 using $\Delta\delta = \delta - \delta^*$.

determined as a function of oxygen activity as shown in Table 1. In order to determine the absolute values of the nonstoichiometry, therefore, it is necessary to evaluate the reference values, δ^* , and the defect structure of the system.

Defect structure of various spinel ferrites, $(Me, Fe)_{3-\delta}O_4$ [$Me = Fe$ (16, 17), Mn (18, 19), Co (20), Cr (21), Ti (22), Mg (14, 15, 23, 24), $CoMn$ (25, 26), and $MnZn$ (27)] has been studied via nonstoichiometry (δ), cationic tracer diffusion coefficient (D^*), and cationic transference number (t_{ion}) measurements. Although there are some reports (11, 28) which claim that the defect structure of spinel ferrites is Schottky disorder on the basis of lattice parameter variation with the nonstoichiometry, it seems to be certain from the results in Refs. (14, 15, 16–27) that the spinel ferrites have Frenkel-defects as the majority type of disorder. If it is the case, the nonstoichiometry (δ) of a spinel ferrite is expressed by (14, 15, 17, 20, 21–26)

$$\delta = [V]^{\circ} \cdot a_{O_2}^{2/3} - [I]^{\circ} \cdot a_{O_2}^{-2/3}, \quad [5]$$

where $[V]^{\circ}$ and $[I]^{\circ}$ are the number of cation vacancies and interstitials, respectively, per lattice molecule corresponding to $a_{O_2} = 1$. (Hereafter, $[V]^{\circ}$ and $[I]^{\circ}$ will be referred to as the defect constant for cation vacancy and interstitial, respectively.) Considering structural similarity, $(Mg_{0.22}Mn_{0.07}Fe_{0.71})_{3-\delta}O_4$ ferrite can also be assumed to have Frenkel-type disorder, and the nonstoichiometry (δ) of $(Mg_{0.22}Mn_{0.07}Fe_{0.71})_{3-\delta}O_4$ ferrite may be represented as Eq. [5]. Therefore, the relative nonstoichiometry ($\Delta\delta$) is given as follows:

$$\Delta\delta = \delta - \delta^* = [V]^{\circ} \cdot a_{O_2}^{2/3} - [I]^{\circ} \cdot a_{O_2}^{-2/3} - \delta^*. \quad [6]$$

The experimental data in Table 1 were fitted to Eq. [6] to obtain $[V]^{\circ}$, $[I]^{\circ}$, and δ^* , which are listed in Table 2, and the

absolute values of δ as calculated from $\Delta\delta$ and δ^* are listed in Table 1 and shown in Fig. 2. The solid lines in Fig. 2 are the best fitted to Eq. [5]. As is seen, the experimental results well satisfy Eq. [5], supporting the validity of Eq. [6]. The nonstoichiometry of $(Mg_{0.22}Mn_{0.07}Fe_{0.71})_{3-\delta}O_4$ amounts to about 0.02 at maximum in absolute magnitude, which justify the validity of the assumption employed in Eq. [3], $\delta/3, \delta^*/3 \ll 1$.

Thermodynamic Calculation

Temperature dependencies of the defect constants for cation vacancy ($[V]^{\circ}$) and interstitial ($[I]^{\circ}$) are shown in Figs. 3 and 4, respectively, which may be best estimated as

$$\ln [V]^{\circ} = (-16.4 \pm 2.2) + \frac{(1.9 \pm 0.3) \times 10^4 \text{ K}}{T} \quad [7]$$

$$\ln [I]^{\circ} = (34.4 \pm 0.5) + \frac{(6.89 \pm 0.07) \times 10^4 \text{ K}}{T} \quad [8]$$

TABLE 2
Defect Constants $[V]^{\circ}$ and $[I]^{\circ}$ Obtained by Nonlinear Fittings of the Experimental Data for $(Mg_{0.22}Mn_{0.07}Fe_{0.71})_{3-\delta}O_4$ at 1000, 1100, and 1200°C to Eq. [7]

T ($^{\circ}\text{C}$)	$[V]^{\circ}$	$[I]^{\circ}$	δ^*
1000	0.27 ± 0.01^a	$(3.5 \pm 0.7) \times 10^{-9}$	0.0013 ± 0.0003
1100	0.081 ± 0.006	$(1.4 \pm 0.2) \times 10^{-7}$	0.0010 ± 0.0004
1200	0.041 ± 0.003	$(4.5 \pm 0.2) \times 10^{-6}$	0.0096 ± 0.0003

^a All of the error values listed are fitting errors.

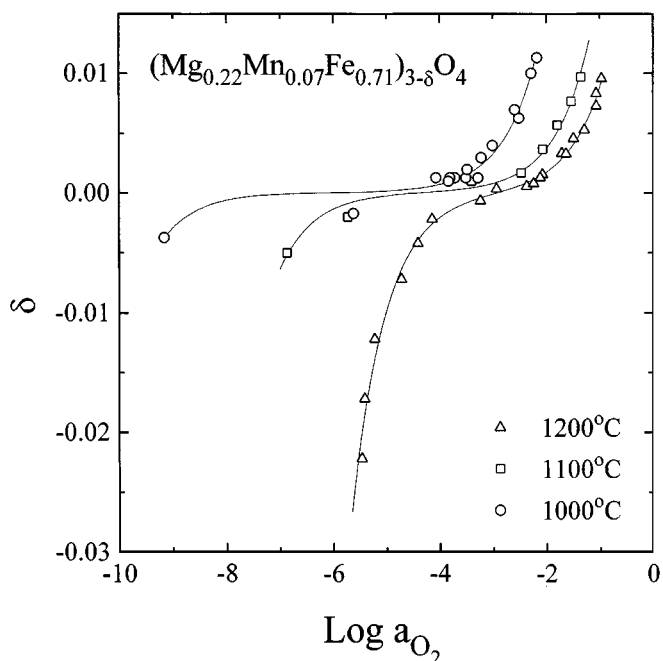


FIG. 2. Nonstoichiometry (δ) of $(\text{Mg}_{0.22}\text{Mn}_{0.07}\text{Fe}_{0.71})_{3-\delta}\text{O}_4$ vs oxygen activity, a_{O_2} , at different temperatures. The solid lines are the best fitted to Eq. [5].

In a spinel structure, there are two kinds of interstices: tetrahedral and octahedral. If cation vacancies are assumed to be present predominantly on octahedral sites, as in

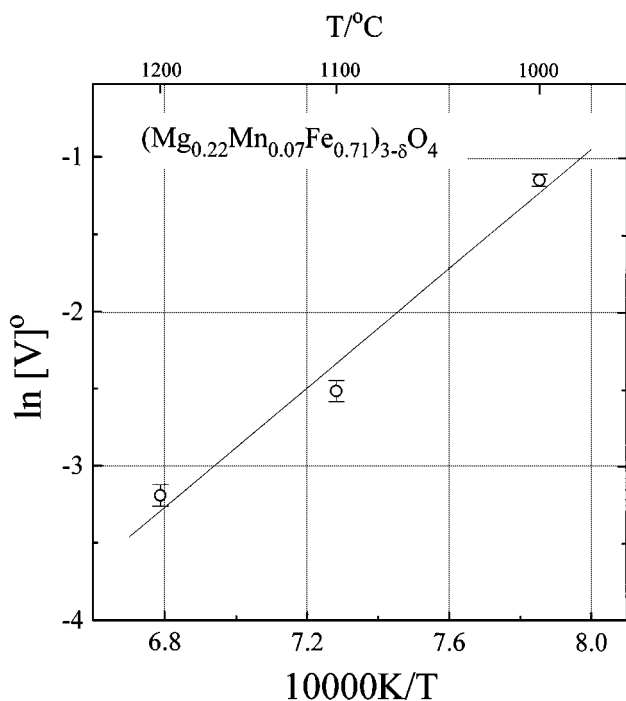


FIG. 3. Temperature dependence of the defect constant for the formation of cation vacancy, $[V]^0$, of $(\text{Mg}_{0.22}\text{Mn}_{0.07}\text{Fe}_{0.71})_{3-\delta}\text{O}_4$.

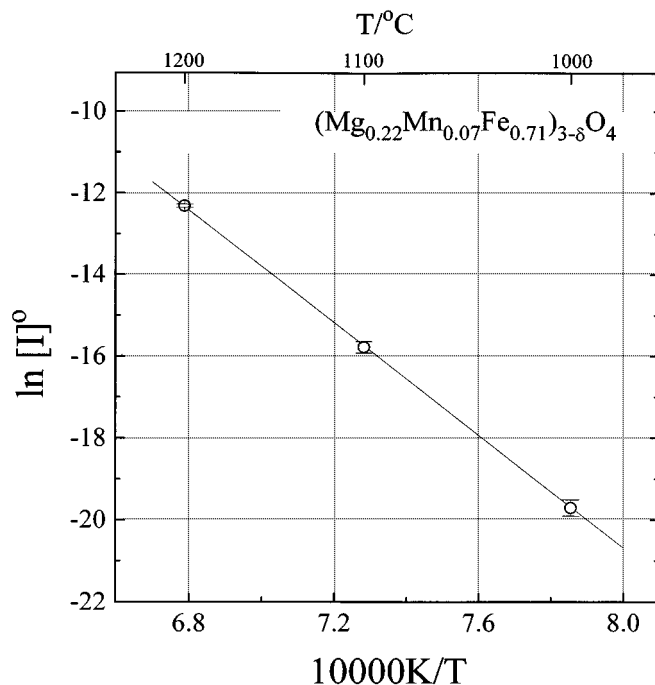
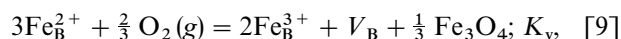


FIG. 4. Temperature dependence of the defect constant for the formation of interstitial cation, $[I]^0$, of $(\text{Mg}_{0.22}\text{Mn}_{0.07}\text{Fe}_{0.71})_{3-\delta}\text{O}_4$.

$\text{Fe}_{3-\delta}\text{O}_4$ (17) and $(\text{Mg}_x\text{Fe}_{1-x})_{3-\delta}\text{O}_4$ (14, 15), they may form via reaction,



where the subscript B denotes the octahedral site and K_V is the reaction equilibrium constant. Applying the mass action law to Eq. [9] on the assumption of ideal dilute solution, the number of cation vacancies per lattice molecule is given by

$$[V_B] = [V]^0 \cdot a_{\text{O}_2}^{2/3}, \quad [10]$$

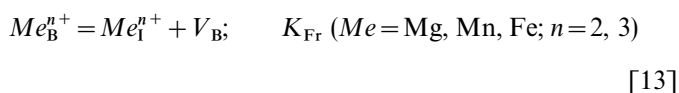
where

$$[V]^0 = K_V \cdot \frac{[\text{Fe}_B^{2+}]_0^3}{[\text{Fe}_B^{3+}]_0^2} \cdot a_{\text{Fe}_3\text{O}_4}^{-1/3}. \quad [11]$$

Here, $a_{\text{Fe}_3\text{O}_4}$ denotes the activity of Fe_3O_4 in $(\text{Mg}_{0.22}\text{Mn}_{0.07}\text{Fe}_{0.71})_{3-\delta}\text{O}_4$, $[\text{Fe}_B^{2+}]_0$ and $[\text{Fe}_B^{3+}]_0$ the number of ferrous and ferric ions, respectively, per lattice molecule on the octahedral sites at $a_{\text{O}_2} = 1$. According to Yoo and Tuller (29), the variations of $[\text{Fe}_B^{2+}]$ and $[\text{Fe}_B^{3+}]$ with temperature are negligible in the temperature range investigated in this study. It then follows from Eq. [11] that

$$\frac{\partial \ln [V]^0}{\partial(1/T)} \cong \frac{\partial \ln K_V}{\partial(1/T)}. \quad [12]$$

As far as the interstitial cations are concerned, there are six possible defects [$Mg_{I(A)}^{2+}$, $Mg_{I(B)}^{2+}$, $Fe_{I(A)}^{2+}$, $Fe_{I(B)}^{2+}$, $Fe_{I(A)}^{3+}$, $Fe_{I(B)}^{3+}$], the subscripts I(A) and I(B) denoting tetrahedrally and octahedrally coordinated interstitial sites, respectively] and six corresponding defect formation reactions should be taken into account. For the sake of simplicity, however, a simplified Frenkel pair formation reaction, where the ionic species and charge state are not distinguished, will be considered as



Applying the mass action law to Eq. [13], one obtains the number of interstitial cations per lattice molecule as

$$[Me_I^{n+}] = K_{Fr} \cdot \frac{[Me_B^{n+}]}{[V_B]} = K_{Fr} \cdot \frac{[Me_B^{n+}]}{[V]^o} \cdot a_{O_2}^{-2/3}. \quad (14)$$

By definition, the defect constant for interstitial cation, $[I]^o$ is then expressed as

$$[I]^o = [Me_I^{n+}]_{a_{O_2}=1} = \frac{[Me_B^{n+}]^o}{[V]^o} \cdot K_{Fr}, \quad [15]$$

where $[Me_B^{n+}]^o$ is the number of Me on the octahedral site per lattice molecule at $a_{O_2} = 1$. Therefore,

$$\frac{\partial \ln K_{Fr}}{\partial (1/T)} = \frac{\partial \ln [V]^o}{\partial (1/T)} + \frac{\partial \ln [I]^o}{\partial (1/T)}. \quad [16]$$

The enthalpy changes for the formation of cation vacancy and Frenkel pair can thus be estimated from the slopes of the straight lines in Figs. 3 and 4 as $\Delta H_V = -158 \pm 25$ kJ/mol and $\Delta H_{Fr} = 416 \pm 6$ kJ/mol, respectively. These values are in agreement within the error range with those for the composition of $(Mg_{0.29}Fe_{0.71})_{3-\delta}O_4$, $\Delta H_V = -182 \pm 3$ kJ/mol and $\Delta H_{Fr} = 360 \pm 140$ eV (30), but a little higher and lower for ΔH_V and ΔH_{Fr} , respectively, than those for $Fe_{3-\delta}O_4$, $\Delta H_V = -198$ kJ/mol and $\Delta H_{Fr} = 522$ kJ/mol (17).

At the inflection point in the plot of δ against $\log a_{O_2}$ in Fig. 2, the $(Mg_{0.22}Mn_{0.07}Fe_{0.71})_{3-\delta}O_4$, ferrite becomes stoichiometric (i.e., $\delta = 0$), and from Eq. [5] the oxygen activity of the stoichiometric composition, $(Mg_{0.22}Mn_{0.07}Fe_{0.71})_3O_4$, is derived as

$$a_{O_2}^* = a_{O_2} (\delta = 0) = \left(\frac{[I]^o}{[V]^o} \right)^{3/4}. \quad [17]$$

In Fig. 5 is shown $a_{O_2}^*$ of stoichiometric $(Mg_{0.22}Mn_{0.07}Fe_{0.71})_3O_4$ at each temperature together with those of

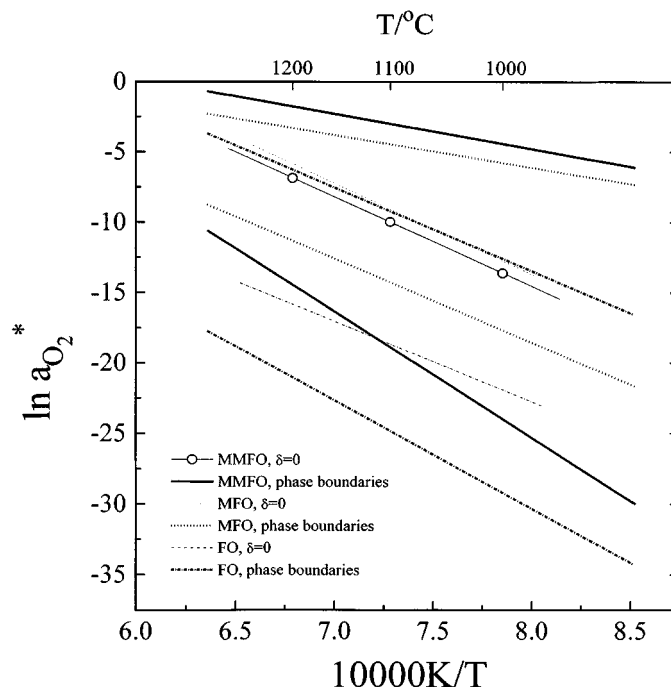


FIG. 5. Oxygen activity of stoichiometric composition, $a_{O_2}^*$, of $(Mg_xMn_yFe_{1-x-y})_3O_4$ as a function of inverse temperature. MMFO, MFO, and FO denote $(Mg_{0.22}Mn_{0.07}Fe_{0.71})_3O_4$, $(Mg_{0.29}Fe_{0.71})_3O_4$, and Fe_3O_4 , respectively. Data for MFO (thin dotted line) and FO (thin dash-dotted line) are calculated ones with $[V]^o$ and $[I]^o$ reported in Refs. (14) and (17), respectively, using Eq. [17]. Phase boundaries of MMFO, MFO, and FO are taken from Refs. (5), (6), and (17), respectively.

$(Mg_{0.29}Fe_{0.71})_3O_4$ and Fe_3O_4 which were calculated with $[V]^o$ and $[I]^o$ reported in the literature (14, 17).

When a metal oxide is in equilibrium with surrounding gas atmosphere, the chemical potential of oxygen in the oxide is equal to that in the gas atmosphere, i.e.,

$$2\mu_o (\text{oxide}) = \mu_{O_2} (\text{gas}). \quad [18]$$

The chemical potential of oxygen in the gas atmosphere is defined by the equation:

$$\mu_{O_2} (\text{gas}) = \mu_{O_2}^o + RT \ln a_{O_2}, \quad [19]$$

where $\mu_{O_2}^o$ is the chemical potential of oxygen at standard state, i.e., $a_{O_2} = 1$. The relative partial molar free energy of oxygen, $\Delta \bar{G}_{O_2}$, is, therefore, given as

$$\Delta \bar{G}_{O_2} = 2\mu_o (\text{oxide}) - \mu_{O_2}^o = RT \ln a_{O_2}. \quad [20]$$

Incorporating Eq. [20] into the free energy expression, $\Delta \bar{G}_{O_2} = \Delta \bar{H}_{O_2} - T\Delta \bar{S}_{O_2}$, we obtain

$$\ln a_{O_2} = \frac{\Delta \bar{H}_{O_2}}{RT} - \frac{\Delta \bar{S}_{O_2}}{R}. \quad [21]$$

TABLE 3

Enthalpy Changes for the Defect Formation Reactions ΔH_V and ΔH_{Fr} , in (Mg_xMn_yFe_{1-x-y})_{3-δ}O₄ and Relative Partial Molar Enthalpy and Entropy of Oxygen, $\Delta \bar{H}_{O_2}$ and $\Delta \bar{S}_{O_2}$, of Stoichiometric (Mg_xMn_yFe_{1-x-y})₃O₄

System	ΔH_V	ΔH_{Fr}	$\Delta \bar{H}_{O_2}$	$\Delta \bar{S}_{O_2}$
(Mg _{0.22} Mn _{0.07} Fe _{0.71}) _{3-δ} O ₄	-158 ± 25	416 ± 6	-529 ± 25	-302.6 ± 1.7
(Mg _{0.29} Fe _{0.71}) _{3-δ} O ₄	-182 ± 3 ^a	360 ± 140 ^a	-540 ± 110 ^c	-320 ± 80 ^c
Fe _{3-δ} O ₄	-198 ^b	522 ^b	-470 ± 140 ^d	-191 ± 9 ^d

Note. ΔH_V , ΔH_{Fr} , and $\Delta \bar{H}_{O_2}$ are in kJ/mole, and $\Delta \bar{S}_{O_2}$ in J/K-mole.

^{a, b} Taken from Refs. [30] and [17], respectively.

^{c, d} Calculated with $[V]^\circ$ and $[I]^\circ$ reported in Refs. [14] and [17], respectively.

Therefore, the slope and intercept of the solid line in Fig. 5 yield relative partial molar enthalpy and entropy of oxygen for the stoichiometric composition (Mg_{0.22}Mn_{0.07}Fe_{0.71})₃O₄, i.e., $\Delta \bar{H}_{O_2}$ and $\Delta \bar{S}_{O_2}$, respectively. They were calculated to be $\Delta \bar{H}_{O_2} = -529 \pm 25$ kJ/mol and $\Delta \bar{S}_{O_2} = -302.6 \pm 1.7$ J/K-mol. Calculating $\Delta \bar{H}_{O_2}$ and $\Delta \bar{S}_{O_2}$ for Fe₃O₄ and (Mg_{0.29}Fe_{0.71})₃O₄ with the data shown in Fig. 5, we could obtain $\Delta \bar{H}_{O_2} = -470 \pm 140$ kJ/mol, $\Delta \bar{S}_{O_2} = -191 \pm 9$ J/K-mol for Fe₃O₄, and $\Delta \bar{H}_{O_2} = -540 \pm 110$ kJ/mol, $\Delta \bar{S}_{O_2} = -320 \pm 80$ J/K-mol for (Mg_{0.29}Fe_{0.71})₃O₄.

All of the thermodynamic quantities extracted from the temperature dependence of the nonstoichiometry of (Mg_{0.22}Mn_{0.07}Fe_{0.71})_{3-δ}O₄ are summarized in Table 3 together with those for Fe_{3-δ}O₄ and (Mg_{0.29}Fe_{0.71})_{3-δ}O₄.

As is seen from the sign of ΔH_V , the cation vacancy formation or oxygen incorporation reactions (Eq. [9]) in (Mg_{0.22}Mn_{0.07}Fe_{0.71})_{3-δ}O₄, (Mg_{0.29}Fe_{0.71})_{3-δ}O₄, and Fe_{3-δ}O₄ are exothermic. Cation vacancy formation in (Mg_{0.22}Mn_{0.07}Fe_{0.71})_{3-δ}O₄, (Mg_{0.29}Fe_{0.71})_{3-δ}O₄, and Fe_{3-δ}O₄ is, thus, suppressed with increasing temperature, and, consequently, nonstoichiometry decreases at constant a_{O_2} as can be seen in Fig. 2. For Mn_{3-δ}O₄, on the contrary, things are totally opposite. Keller and Dieckman (31) measured the nonstoichiometry of α -Mn_{3-δ}O₄ (tetragonally dis-

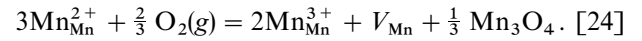
torted spinel structure) and β -Mn_{3-δ}O₄ (spinel structure) in the temperature range of 1000–1350°C via thermogravimetry and concluded that the dominant defect species in both phases are cation vacancies and manganese interstitials, i.e., Frenkel disorder. They presented the temperature dependence of $[V]^\circ$ for both phases as

$$\log K_V(\alpha\text{-Mn}_{3-\delta}\text{O}_4) = 9.43 - \frac{16,350 K}{T} \quad [22]$$

and

$$\log K_V(\beta\text{-Mn}_{3-\delta}\text{O}_4) = 1.58 - \frac{5954 K}{T}, \quad [23]$$

where K_V is the reaction equilibrium constant for the following reaction in each phase



This temperature dependence of K_V for each phase yields ΔH_V as 313 kJ/mol (α -Mn_{3-δ}O₄) and 114 kJ/mol (β -Mn_{3-δ}O₄); i.e., the cation vacancy formation reactions in Mn_{3-δ}O₄ are endothermic. At a fixed oxygen activity, therefore, the nonstoichiometry increases with increasing temperature. It is interesting that the sign of ΔH_V is opposite for the two oxide systems, (Mg_xMn_yFe_{1-x-y})_{3-δ}O₄ [($x + y$) < 1/3] and Mn_{3-δ}O₄, which have similar crystallographic structure and the same defect structure—one is exothermic and the other endothermic. The same feature is found in binary transition metal monoxides, the majority ionic defects of which are cation vacancies. In Table 4 are listed cation vacancy formation reactions for various transition metal oxides and corresponding enthalpy changes. As is seen in Table 4, the transition metal oxides containing Fe as the major components exhibit the exothermicity for cation vacancy formation and the others endothermicity except for Mn_{1-δ}O at lower temperature than 1375°C. Because the cation vacancy formation in the

TABLE 4
Cation Vacancy Formation Reactions and Their Enthalpies for Various Transition Metal Oxides

System	Reaction	ΔH_V° (eV)	Temp. (°C)	Ref.
(Mg _{0.22} Mn _{0.07} Fe _{0.71}) _{3-δ} O ₄	$3\text{Fe}_{\text{B}}^{3+} + \frac{2}{3} \text{O}_2(\text{g}) = 2\text{Fe}_{\text{B}}^{3+} + V_{\text{B}} + \frac{1}{3} \text{Fe}_3\text{O}_4$	-1.64 ± 0.26	1000–1200	Present work
(Mg _{0.29} Fe _{0.71}) _{3-δ} O ₄	$3\text{Fe}_{\text{B}}^{3+} + \frac{2}{3} \text{O}_2(\text{g}) = 2\text{Fe}_{\text{B}}^{3+} + V_{\text{B}} + \frac{1}{3} \text{Fe}_3\text{O}_4$	-1.89 ± 0.03	1000–1200	(14)
Fe _{3-δ} O ₄	$3\text{Fe}_{\text{B}}^{3+} + \frac{2}{3} \text{O}_2(\text{g}) = 2\text{Fe}_{\text{B}}^{3+} + V_{\text{B}} + \frac{1}{3} \text{Fe}_3\text{O}_4$	-2.06	900–1400	(17)
Mn _{3-δ} O ₄	$3\text{Mn}_{\text{Mn}}^{2+} + \frac{2}{3} \text{O}_2 = 2\text{Mn}_{\text{Mn}}^{2+} + V_{\text{Mn}} + \frac{1}{3} \text{Mn}_3\text{O}_4$	2.53	1000–1130	(31)
		0.908	1200–1350	
Fe _{1-δ} O	$2\text{Fe}_{\text{Fe}}^{\times} + \frac{1}{2} \text{O}_2 = (V_{\text{Fe}}\text{Fe}_i V_{\text{Fe}}) + \text{Fe}_{\text{Fe}} + \text{O}_\text{O}^\times$	-2.68	800–1250	(32)
Co _{1-δ} O	$2\text{Co}_{\text{Co}}^{\times} + \frac{1}{2} \text{O}_2 = V_{\text{Co}} + 2\text{h} + \text{CoO}$	1.55	1000–1400	(33)
Ni _{1-δ} O	$\frac{1}{2} \text{O}_2 = \text{O}_\text{O}^\times + V_{\text{Ni}} + 2\text{h}$	2.5	836–1086	(34)
Mn _{1-δ} O	$\frac{1}{2} \text{O}_2 = \text{O}_\text{O}^\times + V_{\text{Mn}} + 2\text{h}$	1.41	> 1375	(35)

transition metal oxides is accompanied by the oxidation of the transition metal ions for charge compensation, the opposite trend in the cation vacancy formation seems to arise from the difference in oxidation potential between Fe and other transition metal ions in the ionic crystal structure. Furthermore, the electron configuration of the transition metal ions in the ionic crystal may affect the temperature dependence of the reaction constants for the cation vacancy formation reactions. It will be interesting and valuable to elucidate the origin of the difference in the enthalpies for the cation vacancy formation in transition metal oxides from the viewpoint of the crystal chemistry, but more detailed information cannot be drawn from the present results.

SUMMARY AND CONCLUSIONS

The nonstoichiometry (δ) of $(\text{Mg}_{0.22}\text{Mn}_{0.07}\text{Fe}_{0.71})_{3-\delta}\text{O}_4$ has been measured as a function of oxygen activity, a_{O_2} , at 1000–1200°C via a solid state coulometric titration technique. The nonstoichiometry isotherms varied sine-hyperbolically with $\log a_{\text{O}_2}$ and shift toward higher oxygen activity as temperature increases, and the oxygen activity dependence of δ was well explained in terms of Frenkel disorder: cation vacancies are predominant at high a_{O_2} and interstitial cations at low a_{O_2} . Absolute values of the nonstoichiometry at each temperature were determined by fitting the experimental data to the equation generally known for spinel oxides and the nonstoichiometry at each temperature could best be estimated as

$$\delta = (0.27 \pm 0.01) \cdot a_{\text{O}_2}^{2/3} - (3.5 \pm 0.7) \times 10^{-9} \cdot a_{\text{O}_2}^{-2/3} \quad \text{at } T = 1000^\circ\text{C}$$

$$\delta = (0.081 \pm 0.006) \cdot a_{\text{O}_2}^{2/3} - (1.4 \pm 0.2) \times 10^{-7} \cdot a_{\text{O}_2}^{-2/3} \quad \text{at } T = 1100^\circ\text{C}$$

$$\delta = (0.041 \pm 0.003) \cdot a_{\text{O}_2}^{2/3} - (4.5 \pm 0.2) \times 10^{-6} \cdot a_{\text{O}_2}^{-2/3} \quad \text{at } T = 1200^\circ\text{C}$$

From the temperature dependence of the defect constants, $[V]^\circ$ and $[I]^\circ$, the enthalpy changes for the formation of cation vacancy (ΔH_V) and Frenkel-defect pair (ΔH_{Fr}) were calculated as $\Delta H_V = -158 \pm 25$ kJ/mol and $\Delta H_{\text{Fr}} = 416 \pm 6$ kJ/mol, respectively. The relative partial molar enthalpy ($\Delta \bar{H}_{\text{O}_2}$) and entropy ($\Delta \bar{S}_{\text{O}_2}$) of oxygen in stoichiometric $(\text{Mg}_{0.22}\text{Mn}_{0.07}\text{Fe}_{0.71})_3\text{O}_4$ were calculated from the temperature-dependence of oxygen activity for stoichiometric composition ($\delta = 0$) and they were $\Delta \bar{H}_{\text{O}_2} = -529 \pm 25$ kJ/mol and $\Delta \bar{S}_{\text{O}_2} = -302.6 \pm 1.7$ J/K-mol.

ACKNOWLEDGMENT

This work has been financially supported by the Ministry of Education Research Fund for Advanced Materials in 1996.

REFERENCES

1. H. L. Tuller, H.-I. Yoo, W. Kehr, and R. W. Scheidecker, in "Advances in Ceramics" (F. Y. Wang, Ed.), Vol. 15, Am. Ceram. Soc., OH, 1985.
2. H.-I. Yoo and H. L. Tuller, *J. Am. Ceram. Soc.* **70**, 388 (1987).
3. H.-I. Yoo and H. L. Tuller, *J. Mater. Res.* **3**, 552 (1988).
4. J.-H. Kim, H.-I. Yoo, and H. L. Tuller, *J. Am. Ceram. Soc.* **73**, 258 (1990).
5. J.-H. Chae, H.-I. Yoo, S.-H. Kang, D.-S. Kang, and B.-D. You, *J. Korean Ceram. Soc.* **32**, 394 (1995).
6. S.-H. Kang, S.-H. Chang, and H.-I. Yoo, *J. Phys. IV* **7-C1**, 253 (1997).
7. A. Goldman, in "Modern Ferrite Technology," Van Nostrand-Reinhold, New York, 1990.
8. P. K. Gallagher, E. M. Gyorgy, and D. W. Johnson, Jr., *Am. Ceram. Soc. Bull.* **57**, 812 (1978).
9. A. Morita and A. Okamoto, in "Ferrites," Proc. 3rd ICF, p. 313, Japan Soc. of Powder and Powder Metallurgy, Tokyo, 1980.
10. T. Tanaka, *Jpn. J. Appl. Phys.* **17**, 349 (1978).
11. H. Inaba, *J. Am. Ceram. Soc.* **78**, 2907 (1995).
12. Nicolas, in "Ferromagnetic Materials," (E. P. Wohlfarth, Ed.), Vol. 2 Chap. 4. North-Holland, New York, 1980.
13. R. A. McCurrie, in "Ferromagnetic Materials—Structure and Properties," p. 152. Academic Press, San Diego, 1994.
14. S.-H. Kang and H.-I. Yoo, *Solid State Ionics* **86-88**, 751 (1996).
15. S.-H. Kang and H.-I. Yoo, *J. Solid State Chem.* **139**, 128 (1998).
16. R. Dieckmann, T. O. Mason, J. D. Hodge, and H. Schmalzried, *Ber. Bunsen-Ges. Phys. Chem.* **82**, 778 (1978).
17. R. Dieckmann, *Ber. Bunsen-Ges. Phys. Chem.* **86**, 112 (1982).
18. P. Franke and R. Dieckmann, *Solid State Ionics* **32**, 817 (1989).
19. P. Franke and R. Dieckmann, *J. Phys. Chem. Solids* **51**, 49 (1990).
20. F.-H. Lu, S. Tinkler, and R. Dieckmann, *Solid State Ionics* **62**, 39 (1993).
21. J. Töpfer, S. Aggarwal, and R. Dieckmann, *Solid State Ionics* **81**, 251 (1995).
22. S. Aggarwal and R. Dieckmann, in "MRS Proceedings," Vol. 369, (G.-A. Nazri, J.-M. Tarascon, and M. Schreiber, Eds.), Vol. 369, pp. 307–312. Materials Research Society, Pittsburgh, PA, 1995.
23. S.-H. Kang, H.-I. Yoo, D.-S. Kang, and B.-D. You, *J. Korean Ceram. Soc.* **31**, 1491 (1994).
24. S.-H. Kang and H.-I. Yoo, *J. Phys. IV* **7-C1**, 247 (1997).
25. F.-H. Lu and R. Dieckmann, *Solid State Ionics* **53-56**, 290 (1992).
26. F.-H. Lu and R. Dieckmann, *Solid State Ionics* **59**, 71 (1993).
27. Y.-I. Jang and H.-I. Yoo, *Solid State Ionics* **84**, 77 (1996).
28. T. Tanaka, *Jpn. J. Appl. Phys.* **13**, 1235 (1974).
29. H.-I. Yoo and H. L. Tuller, *J. Phys. Chem. Solids* **49**, 761 (1988).
30. S.-H. Kang, Ph.D. thesis, Seoul National Univ., Korea, 1998.
31. M. Keller and R. Dieckmann, *Ber. Bunsen-Ges. Phys. Chem.* **89**, 1095 (1985).
32. P. Kofstad, "Nonstoichiometry, Diffusion, and Electrical Conductivity in Binary Metal Oxides." Wiley & Sons, New York, 1972.
33. R. Dieckmann, *Z. Phys. Chem. N. F.* **107**, 189 (1977).
34. Y. D. Tretyakov and R. A. Rapp, *Trans. Metal. Soc. AIME.* **245**, 1235 (1969).
35. A. Z. Hed and D. S. Tannhauser, *J. Chem. Phys.* **47**, 2090 (1967).